

Early Detection of Anemia : A well-developed system using machine learning model

Belnekar Janhavi¹, Dube Anuj Soumendra², Kothari Moksha³

^{1,2,3} Student,
Information Technology,
Thakur College of Engineering and Technology
Mumbai, India

Abstract

Anemia, characterized by a deficiency of red blood cells or hemoglobin, remains a global public health concern, particularly in resource-limited regions where access to advanced diagnostic tools is limited. The essence of this work lies in the comprehensive evaluation and analysis of ML models like Convolutional Neural Networks, Logistic Regression, and Gaussian Blur algorithm on publicly available dataset of 710 images of the conjunctiva for pallor analysis. This endeavor aims to furnish the ongoing efforts to improve anemia detection and healthcare access, especially in underserved communities. The implications of this work extend to early intervention and prevention of anemia-related health complications.

Keywords—*pallor analysis, ML models, healthcare access*

I. INTRODUCTION

This research paper presents a task-critical implementation of Convolutional Neural Networks (CNN), Logistic Regression and Gaussian Blur algorithm in computer vision. CNNs are a core deep learning architecture widely used in computer vision. They are designed to automatically and adaptively learn hierarchical features from data, making them highly effective for tasks such as image classification, object detection, and image segmentation. Deep learning techniques have consistently demonstrated significant progress and efficiency in the field of semantic segmentation. Anemia, moving nearly 33% of the global state, presents a important fitness challenge, particularly with youngsters and pregnant daughters. Iron imperfection stands as a chief cause, contributing to 42% of emptiness cases. The prompt discovery of anemia is critical to check the risk of irrevocable organ damage. This study intends a creative non-obtrusive approach, utilizing machine intelligence algorithms to resolve images of palms, fingernails, and conjunctiva. The determined search out overcome support limitations guide unoriginal chlorosis detection orders.

By combining the power of machine learning, image analysis and mobile technology, we present a viable solution that has the potential to revolutionize anemia screening and diagnosis, particularly in resource-constrained settings. This research holds the promise of significantly improving health care access and outcomes for individuals affected by anemia and offers a ray of hope in the ongoing global battle against this pervasive health problem.

II. LITERATURE SURVEY

In recent research, computerized algorithms, particularly machine learning, have shown high accuracy in estimating hemoglobin (Hb) levels and diagnosing medical conditions like anemia # [1]. Various algorithms, including support vector machines (SVM), k-nearest neighbors (k-NN), Bayesian networks, artificial neural networks (ANN), and decision tree classifiers, have been employed for classification. Studies using conjunctiva images of the eyes have demonstrated that the choice of algorithm depends on the specific problem domain # [2]. Non-invasive techniques utilizing clinical symptoms based on fingernails and palm images, as well as conjunctiva images, have shown promise. Different studies have explored the use of machine learning techniques such as ANN, SVM, decision tree, Naïve Bayes, K-NN, and rule-based approaches for anemia detection. The conjunctiva of the eye has been a focus, with SVM achieving 78.90% accuracy # [3], LS-SVM reaching 85% precision, and 98.96% accuracy. Deep learning approaches, including a three-tier deep convolutional fused network, achieved accurate anemia severity prediction.

By utilizing non-invasive methods, healthcare professionals can gain new insights into understanding individual emotional states, leveraging this information for personalized treatment plans. Moreover, the utilization of advanced technologies like the three-tier deep convolutional fused network highlights the immense power of deep learning approaches in predicting the severity of anemia, potentially revolutionizing the early detection and management of this condition. Together, these advancements hold promise for improving diagnosis and treatment outcomes in various medical fields.

Several studies compared the conjunctiva's color with blood parameters and patient attributes, resulting in varied accuracy levels. A novel pipeline based on sclera and blood vessel color achieved 86.4% accuracy. Convolutional neural network (CNN) models, including one with batch normalization layers, demonstrated cost-effective and controllable applications with accuracy up to 89.33%. Other studies explored the application of ANN for Hb level estimation and achieved a sensitivity of 95.50%. Comparisons with laboratory tests showed promising results, with sensitivity and specificity ranging from 77.58% to 91.89%. Some studies proposed using the conjunctiva alone, while others recommended combining it with the palpable palm for increased reliability # [4]. Additionally, an automated system for cataract disease detection using fundus images achieved high accuracy with deep learning architectures.

Despite the advancements, gaps in the related works include the small size of datasets, lack of image augmentation, and the use of single models or features # [4, 5]. This study addresses these gaps by applying five machine learning models to a dataset of 710 conjunctivae, palpable palm, and fingernail images, comparing their performance in detecting anemia in children aged 6–59 months. Non-invasive techniques, especially using conjunctiva images, have proven efficient and cost-effective in diagnosing medical conditions like anemia. This study contributes by comparing the performance of different body features (conjunctiva, palpable palm, and fingernails) in anemia detection. In conclusion, recent research highlights the effectiveness of computerized algorithms, particularly in machine learning, for accurately estimating hemoglobin (Hb) levels and diagnosing anemia. Various successful algorithms, such as SVM, k-NN, Bayesian networks, ANN, and decision tree classifiers, have been applied, with the choice depending on the specific problem domain. Conjunctiva images of the eyes have emerged as valuable in non-invasive techniques, incorporating clinical symptoms from fingernails and palm images. Several studies focused on diverse machine learning techniques for anemia detection, particularly emphasizing conjunctiva images. SVM achieved 78.90% accuracy, LS-SVM reached 85% precision, and a unique approach leveraging emotional posts on Twitter achieved an impressive 98.96% accuracy. Deep learning approaches, like a three-tier deep convolutional fused network, demonstrated precise anemia severity prediction. Convolutional neural network (CNN) models, incorporating batch normalization layers, achieved up to 89.33% accuracy in Hb level estimation.

This study addresses gaps in existing research on anemia detection, utilizing a dataset of 710 images of conjunctiva, palpable palm, and fingernails. Employing five machine learning models, the research emphasizes the efficiency and cost-effectiveness of non-invasive techniques, particularly conjunctiva images, in diagnosing anemia in

children aged 6–59 months. The findings contribute by systematically evaluating the performance of various body features, offering insights for future research and clinical applications.

III. METHODOLOGY

This study was divided into three phases: gathering and preprocessing the dataset, training, and validating the models using the dataset, and applying cross-validation to prevent overfitting. This means that for anemia to be detected, the dataset goes through three phases or steps.

Technique for gathering data:

The data collection system used Kobo Collect on Samsung Galaxy Tab 7A tablets. Biomedical scientists from the University of Energy and Natural Resources, Ghana, captured patient biodata and images (conjunctiva, palm, fingernails), uploaded to cloud storage. The study had ethics approval (Reference: CHRE/CA/042/22). Image capture involved specific methods, like pulling the lower eyelid and stretching palms. Flashlights were off during capture. Images underwent triangle thresholding and segmentation using CIE Lab* color spaces. Data augmentation increased dataset size. Data were collected from 10 health facilities, focusing on children aged 5–59 months. Anemia classification used Hb values (<11 g/dL: anemic, >=11 g/dL: non-anemic). Illustrations included sample images and raw datasets. The study taken moral authorization (Reference: CHRE/CA/042/9), and cognizant consent was obtained from persons or guardians before enrolling minor partners in dossier group.

Images of the conjunctiva were captured by slightly pulling the lower eyelid with the thumb and index finger. For palm images, scientists held the child's hand, stretched the palm through the fingers, and captured the image. Fingernail photos were taken by holding the participant's wrist. To prevent gleam effects, flashlights were turned off during image capture, ensuring consistent image quality and eliminating ambient light influence. By turning off spotlights during image capture, this technique effectively eliminates the influence of ambient light in pictures. This not only reduces shine effects but also significantly improves the model's object recognition and classification capabilities. The approach ensures that datasets of photographs are entirely free from ambient light effects, contributing to enhanced image quality. be used. Other font types may be used if needed for special purposes.

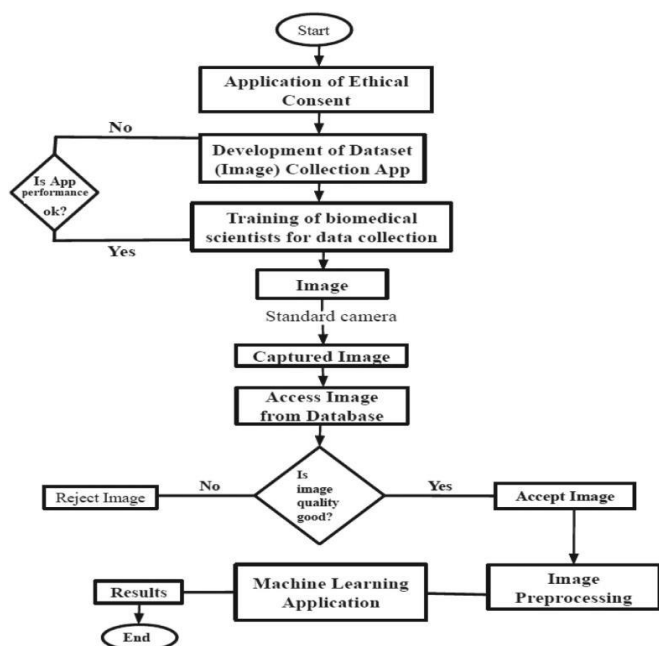


FIGURE 1: A flowchart showing the flow of work in the proposed models.#[12]

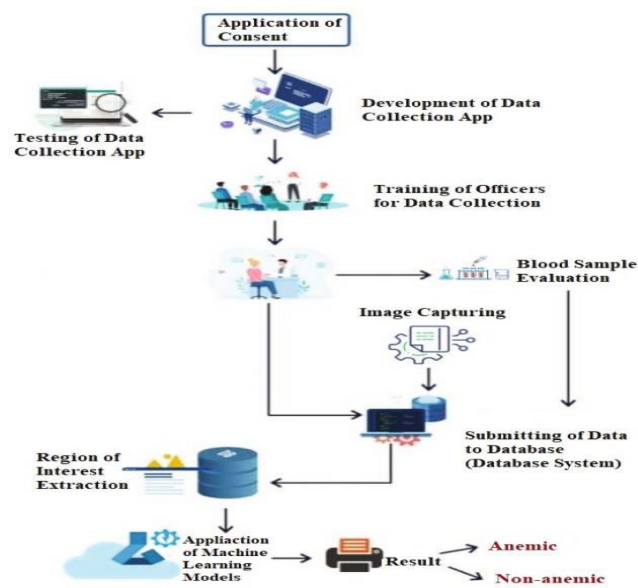


FIGURE 2: A conceptual framework for the proposed methodology.#[12]

3.1. Image Augmentation:

In machine learning, higher accuracy is often achieved by training models on large datasets, as small datasets may lead to overfitting. Overfitting occurs when a model learns the training data too well and fails to generalize to new, unseen data. To address this, image augmentation techniques are employed, involving artificial generation of new data by applying procedures like rotation, shift, flip, and translation to existing images.

Phase 1: Image Augmentation of the Dataset (Images)

To increase the size of the original datasets, an image augmentation technique was applied on the original dataset. This was done because the use of inadequate data could result in overfitting # [6]. The use of image or data augmentation increases the performance of machine learning models. This is because the utilization of image augmentation increases the size of the dataset to enable the models to train with huge dataset sizes or samples and enhance the avoidance of overfitting # [6]. The rotation, flipping and translation image augmentation technique was applied on the original.

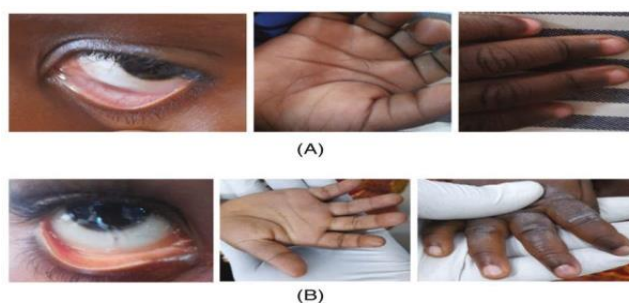


FIGURE 3: Raw images of the conjunctiva of the eyes, palpable palm, and color of the fingernails, where (A) is for non-anemic images and (B) is for anemic images.#[12]

Phase 2. Calculating the RGB and HB Levels of the Extracted ROI: Once the ROI conjunctiva, palm and fingernail has been detected, extracted, and saved as a new image, we compare the final Shape to a set of trained, precisely extracted data to validate and verify it is indeed a data we extracted. The conjunctiva's, palms, and fingernail's Hb level would then have to be calculated. This will be accomplished by extracting the red, blue, and green pixels from the image. Next, we computed the mean of each of the extracted hues, that is, the mean of all the red values, the mean of all the green values and the mean of all the blue values.

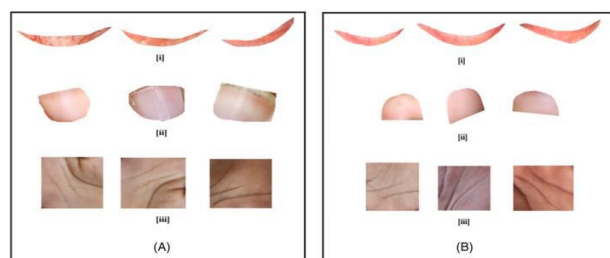


FIGURE 4: Sample of extracted images where (A) are anemic images and (B) are non-anemic images. (i)–(iii) are conjunctiva of the eyes, the color of the fingernails, and the palpable palm respectively, for both (A) and (B) (anemic and non-anemic) images.#[12]

Rotation: In the turn of the figure improving, the real figure is alternated 90°, and 270° to gain the artificial countenance accompanying the principles of the mean force of the concept staying the same the locating of the countenance's changes. The numerical model for turn representation augmentation is registered in Equations (1)–(5). The turn angle θ for the equating for the new matches of a pel is delineated as:

$$x' = x \cos \theta - y \sin \theta \quad (1)$$

$$y' = x \sin \theta + y \cos \theta \quad (2)$$

in an antagonistic-opposite of left turn. In an analogous expression, the position of all pel (x' , y') in the new countenance may be written as a heading and the turn mold:

$$\begin{bmatrix} x' \\ y' \end{bmatrix} = \begin{bmatrix} \cos \theta & -\sin \theta \\ \sin \theta & \cos \theta \end{bmatrix} \begin{bmatrix} x \\ y \end{bmatrix} \quad (3)$$

The turn (x_0 , y_0) is the matches (0, 0) point of root that rotates at the middle of the representation or about the point. For an concept or a pel to alternate about a point (x_0 , y_0) internally the equation is articulated as:

$$x' = x_0 + (x - x_0) \cos \theta + (y - y_0) \sin \theta. \quad (4)$$

$$y' = y_0 + (x - x_0) \sin \theta + (y - y_0) \cos \theta. \quad (5)$$

The pixel at the position (x_0 , y_0) is the only pixel that does not move from its position. If an additional image is intended from the original image one, x and y then describe the equation which needs to be solved.

3.2.2 Flipping:

For the augmentation of various forms of fake images, the original countenances maybe across or across flipped as the locating concerning this movement is changed, while the facial characteristics and components of the principles of the mean force wait unaltered.

Flipping the image results in its placement outside the original figure. When a mirrored image is needed along the y -axis, it requires an additional translation by the image height. The mathematical models for this flipping technique are defined in Equations (6)–(7).

$$x' = x, \quad (6)$$

$$y' = y_{\max} - y. \quad (7)$$

The movements only keep integers of the coordinates and the borders of the countenance which are new expected usually equal to the traditional figure margins outside some break.

3.2.3 Translation

The ROI of real faces exhibits slight variations in both X and Y directions. Translation does not alter the mean intensity characteristics of the facial features. The

numerical models for interpretation in countenance improving are recruited in Equations (8) and (9).

$$x' = x + xT, \quad (8)$$

$$y' = y + yT, \quad (9)$$

Images were augmented through rotation, flipping, and translation, excluding operations that heavily impact mean intensity, like Gaussian and cropping. The final conjunctiva, palpable palm, and fingernails datasets were created post-augmentation. A random split assigned 70% for training, 10% for validation, and 20% for testing. All datasets had consistent sizes and originated from the same patient; removing one image resulted in the exclusion of all images from that patient.

3.3 Machine learning models utilized for the study

3.3.1 Decision trees: Decision trees, effective for analyzing multiple variables, use a branch-like structure where data splits based on various mechanism. # [2] Each branch represents attribute values, and nodes represent attributes. The binary tree has a minimum of 10 instances for each leaf, at least 100 trees, and subsets smaller than 5 are not divided.

3.3.2 Naïve Bayes: Naïve Bayes predicts classes using probability and is a probabilistic classifier with strong independence assumptions. Notably, it often generalizes effectively without requiring hyperparameter adjustments.

3.3.3 k-nearest neighbor (k-NN) algorithm: K-NN is a versatile algorithm suitable for both regression and classification. Despite potential slowdowns with larger datasets, its simplicity and easy implementation are commendable. In this case, K-NN employed 100 neighbors, Euclidean metric with uniform weight, and $k=2$ for the nearest neighbor in the class. It calculates distances between feature vectors and nearest neighbors, generating synthetic data points with slight variations to avoid duplicates.

3.3.4 Support vector machine (SVM): SVMs, a popular classification tool, integrate elements from various methods, assuming separable data. In this instance, the Sigmoid function was used with 100 iterations, a cost parameter (c) of 100, and an epsilon of regression (ϵ) set to 1.10, with a numerical tolerance of 0.1000.

3.3.5 Convolutional neural network: In CNNs, features are identified through filter application, employing a kernel edge with differential values for effective categorization. Training utilizes AlexNet, employing SGD optimization, ReLu activation (regularized with $a=0.0001$), and a maximum iteration of 10. The activation function is crucial for signal transformation, preventing linear regression and facilitating training of complex models.

3.4 Anemia detection condition: This text delves into the intricate use of CIE L*a*b* color space in medical image analysis, specifically targeting hemoglobin level assessment.

1. Image Processing: - ROIs extraction and transformation into CIE L*a*b* color space.

2. Color Correlation: - A* component in CIE L*a*b* shows a robust correlation with hemoglobin levels. - Higher Hb levels associated with $a^* > 160$; lower levels correspond to $a^* < 142.44$.

3. CIE L*a*b* Advantages: - Device-independent image representation for accurate human vision simulation. - Efficient in capturing systematic color changes over time.

4. Perceptual Analysis: - Euclidean distance in L*, a*, b* coordinates for calculating perceptual differences. - L* denotes lightness, while a* and b* represent color channels.

5. Color Components System: - Cartesian coordinates (a*, b*) depict nonalignment as gray. - Red components align with the a* axis; opponent colors (yellow and blue) with b*.

6. Image Filtering Techniques: - Translation of RGB triplets to CIE L*a*b*. - Optimal detection involves combining a*, b*, and G (green) values. - Filtering ensures consideration of specific pixel ranges for accurate pallor assessment.

7. Mathematical Models: - Equations (10)–(13) provide models for CIE L*a*b* color space.

$$L^* = 116f(Y/Y_n) - 16, (10)$$

$$a^* = 500\{f(X/X_n) - f(Y/Y_n)\}, (11)$$

$b^* = 200\{f(X/X_n) - f(Z/Z_n)\}, (12)$, where $f(s) = s/3$, for $s > 0.008856$. And $f(s) = 7.787s + 16/116$, for $s \leq 0.008856$. The color difference ΔE between two colors in the CIE L*a*b* (CIELAB) color space is: $\Delta E = \sqrt{(L^*_2 - L^*_1)^2 + (a^*_2 - a^*_1)^2 + (b^*_2 - b^*_1)^2}, (13)$, where the ΔE unity value denotes a just noticeable difference.

8. Color Difference Computation: - Equation (13) computes color difference (ΔE) in CIE L*a*b*. This study focuses on using CIE L*a*b* color space to discern hemoglobin-related distinctions in medical images, emphasizing its role in precise and meaningful analysis.

3.5 Experimental setup :The study detected anemia using conjunctiva, palm, and fingernail color images from 710 participants, augmented to 2635 images each. The dataset was split into training (70%), validation (10%), and test (20%) sets with 10-fold cross-validation. For anemia detection, CNN utilized SGD optimization, ReLU activation (with $\alpha = 0.0001$). SVM employed Sigmoid, 100 iterations, $c = 100$, $\epsilon = 1.10$, and tolerance = 0.1000. k-NN had 100 neighbors, Euclidean metric, and uniform weight. Decision

tree: min instances in leaves, no split for subsets < 5 , and 100 trees. Orange, a data mining tool on Windows 11, with an Intel Core i3 processor, 4GB RAM, and SSD, was employed. Previous studies by Naik and Samant and Verma and Arjun confirmed Orange's efficacy in disease detection (anemia, diabetes, liver disorder).

3.6 Performance measures :The study evaluated anemia detection models using key metrics (Accuracy, Recall, Specificity, Precision, AUC, F1-score) and 10-fold validation. Formulas (14)–(19) were applied, utilizing TP, TN, FN, P, R, and TNR. These metrics gauged the models' accuracy in identifying positive and negative instances, considering trade-offs between sensitivity, specificity, and overall effectiveness.

$$\text{Accuracy} = (TP + TN) / (TP + TN + FP + FN), (14)$$

$$\text{Recall} = TP / (TP + FN), (15)$$

$$\text{Specificity} = TN / (TN + FP), (16)$$

$$\text{Precision} = TP / (TP + FP), (17)$$

$$\text{AUC (TPR)} = TP / (TP + FN), (18)$$

$$\text{F1 - score} = 2(P.R) / (P + R), (19)$$

IV. RESULTS AND ANALYSIS

After training, validating, and testing, the proposed models demonstrated significant results. The CNN achieved high accuracy: 98.45% on conjunctiva, 98.33% on fingernail color, and 99.12% on palpable palm. SVM had lower accuracy: 89.45% on conjunctiva, 92.96% on fingernail color, and 95.34% on palpable palm. Details and evaluation metrics are presented below, with graphical representations in Figures 4-6, showcasing the models' performance.

4.1. Discussion:

The study aimed to detect anemia using medical images of conjunctiva, palpable palm, and fingernail color from 710 participants. Models were trained, validated, and tested, showing significant results. Naïve Bayes achieved the highest accuracy (98.96%) on palpable palm, while CNN had 99.12%. SVM had the lowest accuracy (95.34%). No significant variations were observed between fingernail color and conjunctiva images. The palm was found to be the most effective in detecting anemia, as supported by previous studies. The extensive and diverse dataset used in this study, publicly available for future research, contributed to its significance. The results emphasized the palm's accuracy, particularly in children under 6, and highlighted CNN's superior performance in conjunctiva and fingernail color detection. Naïve Bayes performed best on the palpable palm.

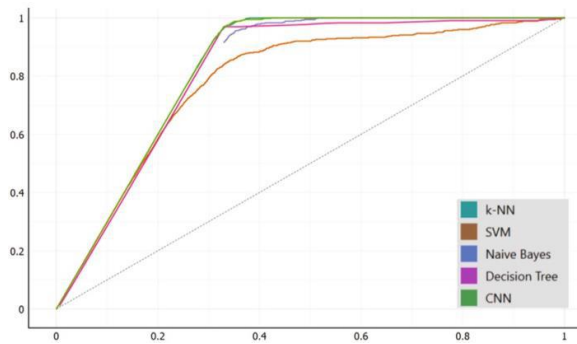


FIGURE 4: AUC curve of the conjunctiva of the eyes for anemia detection.#[12]

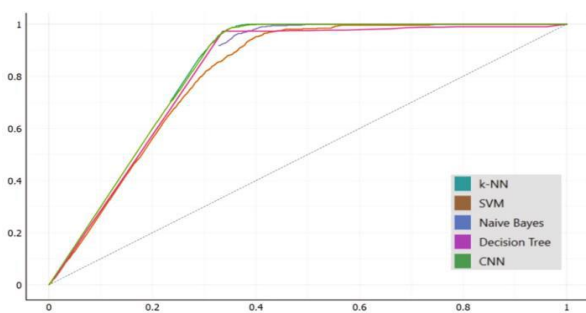


FIGURE 5: AUC curve of the fingernails in anemia detection.#[12]

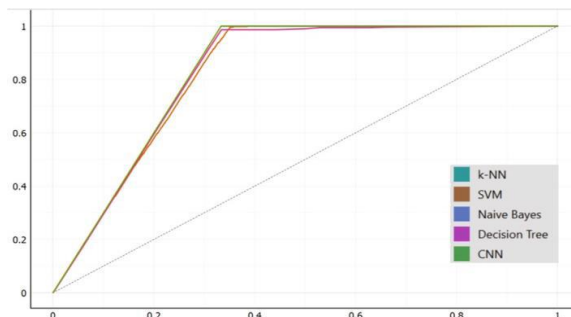


FIGURE 6: AUC curve of the palm in anemia detection.#[12]

4.2.Conclusion :

This item proposed to discover iron deficiency lifelessness, equating machine intelligence models (CNN, Naïve Bayes, resolution tree, k-NN and SVM) act accompanying the use of healing concepts. The models were prepared, validated, and proven on representations of the conjunctiva of analysis, real palm, and color of the fingernails. The CNN had a bigger veracity than all the models when proven on the fingernails, obvious touch, and conjunctiva images. The results got for one model show that the CNN is strong and acts better than Naïve Bayes, conclusion tree, k-NN and SVM in emptiness discovery and the concrete touch is one of the trustworthy human physiognomies for chlorosis

discovery in minors due to allure taller discovery veracity. Furthermore, the performance of the models on the touch had a bigger veracity than that of the fingernails and conjunctiva when proven accompanying the data set. The touch is plain to analyze distinguished to the eyes, that is questioning to approach the conjunctiva and the ROI, specifically for offsprings below 6 age whose eyes can frequently experience dropping. Additionally, minors’ eyes would be unlocked to take pictures or test the conjunctiva of analysis straightforwardly. There is a chance that someone’s finger could infiltrate their eyes. This maybe a potential contamination beginning. The accomplishment of the models would have a great affect the well-being abilities having to do with the detection of iron-imperfection chlorosis on account of the influence and adept performance of the projected models. The large acting of the models acquired by this study would have a great affect strength convenience general, particularly in health conveniences in country Ghana place approach to fitness facilities, supplies or money and energy experts is scarce. However, this study is restricted to the incident and arrangement of a movable request to enhance allure habit, this hopeful deliberate a future work. Future works would acknowledge the growth of a travelling request at which point the proposed models grown hopeful joined to reinforce easy approach and use.

Using Conjunctiva of Eyes

S/N	Algorithm	Accuracy	F1-Score	AUC	Precision	Recall
1	CNN	98.45	97.63	99.93	97.64	97.63
2	Naive Bayes	94.94	92.24	97.74	92.64	91.84
3	Decision Tree	97.32	96.02	97.70	93.67	98.49
4	K-NN	97.96	96.86	99.86	97.60	96.13
5	SVM	89.45	84.53	92.16	81.34	87.98

Using FingerNails

S/N	Algorithm	Accuracy	F1-Score	AUC	Precision	Recall
1	CNN	98.33	97.54	99.93	97.64	97.44
2	Naive Bayes	94.94	92.35	98.01	91.96	92.75
3	Decision Tree	97.18	95.61	97.59	98.41	92.96
4	K-NN	97.89	96.82	99.53	96.21	97.44
5	SVM	92.69	88.62	97.08	91.02	86.35

Using Palm

S/N	Algorithm	Accuracy	F1-Score	AUC	Precision	Recall
1	CNN	99.12	99.89	99.95	99.79	99.98
2	Naive Bayes	98.96	99.97	99.98	99.97	99.93
3	Decision Tree	98.29	98.97	99.38	98.77	99.18
4	K-NN	98.92	99.89	99.98	99.79	99.92
5	SVM	95.34	94.59	98.97	95.99	99.23

V. FUTURE SCOPE:

Developing an offline model to detect anemia through fingernail pictures is a promising solution for healthcare challenges in underserved regions with limited network access. It leverages technology to enhance diagnostic capabilities and improve healthcare outcomes in resource-constrained environments, addressing the lack of consistent internet connectivity in remote areas.

VI. ACKNOWLEDGEMENT:

We extend our heartfelt gratitude to Dr. Sangeeta Vhatkar for her generous and invaluable assistance in the successful completion of this project and her indispensable contributions to the research paper.

VII. REFERENCES

- [1] Dimas Chaerul Ekty Saputra (2023), A New Artificial Intelligence Approach Using Extreme Learning Machine as the Potentially Effective Model to Predict and Analyze the Diagnosis of Anemia. 11(5), 697; <https://doi.org/10.3390/healthcare11050697>
- [2] Roychowdhury S, Sun D, Ren J, BihisM, Hage P, Rahman H.(2017).Screening pallor site images for anemia-like pathologies. Proceedings of the IEEE International Conference on Biomedical Health Informatics
- [3] Collings S, Thompson O, Hirst E, Goossens L, George A, Weinkove R (2016). Non-invasive detection of anaemia using digital photographs of the conjunctiva. <https://doi.org/10.1371/journal.pone.0153286>.
- [4] Appiahene P, Asare JW, Donkoh ET, Dimauro G, Maglietta R. (2023). Detection of iron deficiency anemia by medical images: a comparative study of machine learning algorithms. <https://doi.org/10.1186/s13040-023-00319-z>.
- [5] Bauskar S, Jain P, Gyanchandani M. (2019) A noninvasive computerized technique to detect anemia using images of eye conjunctiva. Pattern Recogn Image Anal <https://doi.org/10.1134/s1054661819030027>.
- [6] Jain P, Bauskar S, Gyanchandani M(2023). Neural network based non-invasive method to detect anemia from images of eye conjunctiva. IntJ Imaging Syst. doi:10.1002/ima.22359
- [7] Tamir A, Jahan CS, Saif MS, et al(2017). Detection of anemia from image of the anterior conjunctiva of the eye by image processing and thresholding. Proceedings of the 2017 IEEE Region 10 Humanitarian Technology Conference. doi:10.1109/R10-HTC.2017.8289053
- [8] Dimauro G, Caivano D, Girardi F(2018). A new method and a non-invasive device to estimate anemia based on digital images of the conjunctiva. IEEE Access. 2018;6:4696846975. doi:10.1109/ACCESS.2018.286710
- [9] Peksi NJ, Yuwono B, Florestiyanto MY(2021). Classification of anemia with digital images of nails and palms using the naive Bayes method.
- [10] Emmanuel DG, David OO, Stephen JB (2022). Deep Convolutional Neural Network Model for Detection of Sick Cell Anemia in Peripheral Blood Images. Commun Phys Sci. 2022;8(1):9-22.
- [11] Sevani N, Fredicia F, Persulesy GBV (2018). Detection anemia based on conjunctiva pallor level using k-means algorithm. IOP Conf Ser Mater Sci Eng. doi:10.1088/1757-899X/420/1/012101
- [12] Justice Williams Asare, Peter Appiahene, Emmanuel Timmy Donkoh, Giovanni Dimauro.(2023) Iron deficiency anemia detection using machine learning models: A comparative study of fingernails, palm and conjunctiva of the eye images. <https://doi.org/10.1002/eng2.12667>